Role of higher-order spatial correlation during colloidal self-assembly

Felix Lehmkühler
ESRF-EBS Coherence Workshop
September 2019

HELMHOLTZ RESEARCH FOR GRAND CHALLENGES

DESY.

X-ray Cross Correlation Analysis (XCCA)

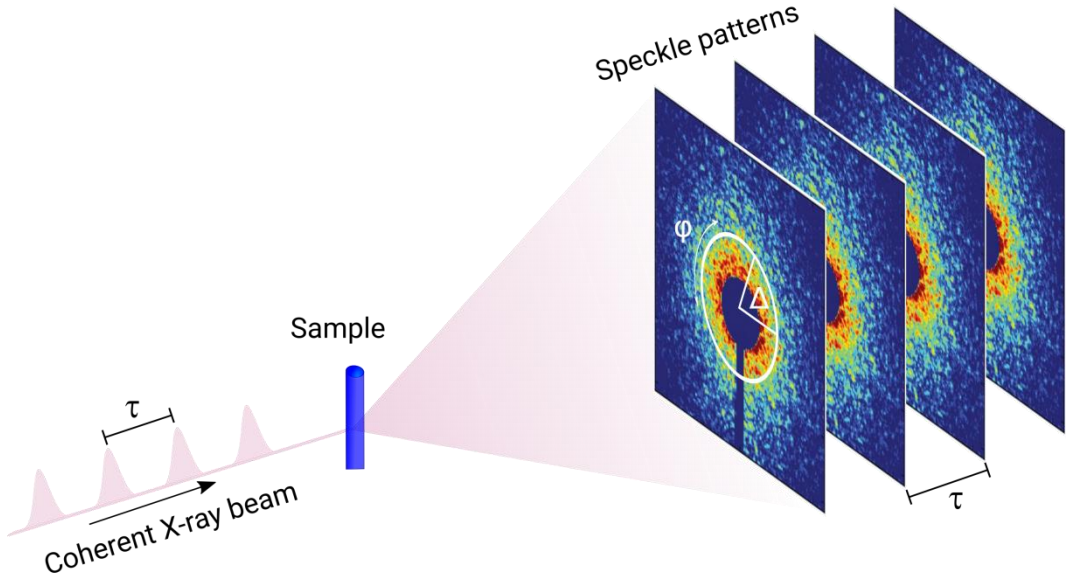

$$\mathbf{C}(\mathbf{Q},\mathbf{Q}',\mathbf{t},\mathbf{t}') \equiv \langle \boldsymbol{I}(\boldsymbol{Q},\boldsymbol{t})\boldsymbol{I}(\boldsymbol{Q}',\boldsymbol{t}')\rangle_{\text{ensemble}}$$

$$\sim \int\int\int\int \boldsymbol{e}^{-i\boldsymbol{Q}(\boldsymbol{r}-\boldsymbol{s})-i\boldsymbol{Q}'(\boldsymbol{r}'-\boldsymbol{s}')}\, \boldsymbol{g}_4(\boldsymbol{r},\boldsymbol{s},\boldsymbol{t},\boldsymbol{r}',\boldsymbol{s}',\boldsymbol{t}')$$

with $g_4(r,s,t,r',s',t') \sim \langle \rho(r,t)\rho(s,t)\rho(r',t')\rho(s',t')\rangle$

→ Pair correlations → static structure factor **SAXS**

$S(Q) \sim \langle I(Q,\varphi,t\rangle_{t,\varphi}$

→ Local, transient symmetries **XCCA**

$C \equiv C_{Q,Q'}(\Delta) \sim \langle I(Q,\varphi)I(Q,\varphi+\Delta)\rangle_{\varphi}$

(e.g. molecular fluids,…)

→ Fluctuations **XPCS**

$C \equiv C_Q(\tau) \sim \langle I(Q,t)I(Q,t+\tau)\rangle_t$

(accompanying equilibrium and non-equilibrium dynamics)

XCCA

Cross-correlation function

$$C(q,\Delta) = \frac{\langle I(q,\varphi)I(q,\varphi+\Delta)\rangle_\varphi - \langle I(q,\varphi)\rangle_\varphi^2}{\langle I(q,\varphi)\rangle_\varphi^2}$$

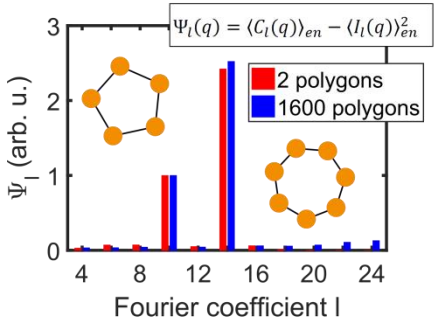

XPCS

Intensity-intensity time autocorrelation function

$$g_2(q,\tau) = \frac{\langle I(q,t)I(q,t+\tau)\rangle_t}{\langle I(q,t)\rangle_t^2}$$

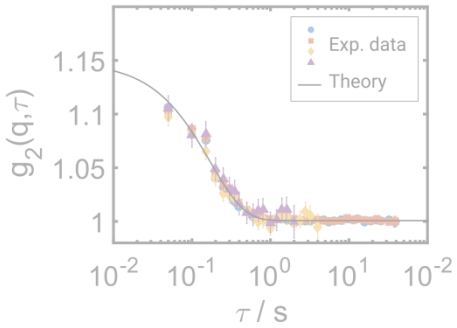

Nanoparticle superstructure formation

Self-assembly and beyond

- Nanoparticle supercrystals with applications in electronics, optoelectronics, as sensors, …
- **Standard route: self-assembly**
  - Solvent evaporation (e.g. drop cast)
  - Sedimentation
  - Solvent destabilization
- Model for crystallisation / phase transitions

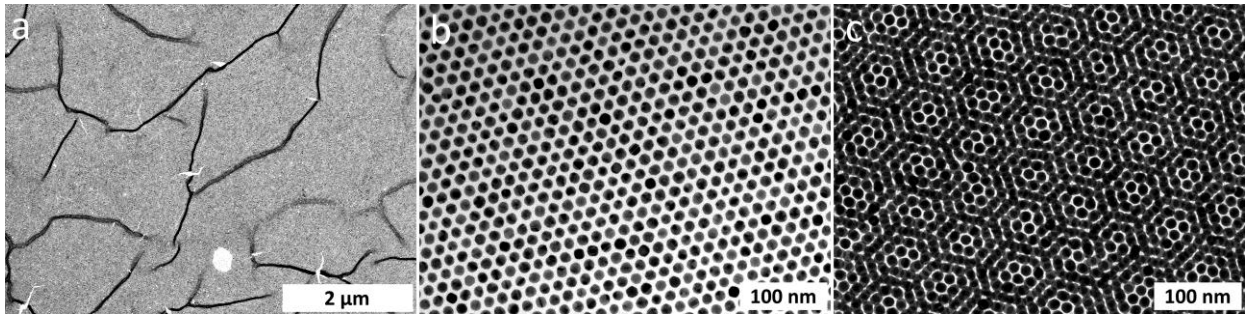

Langmuir 33, 14437 (2017)

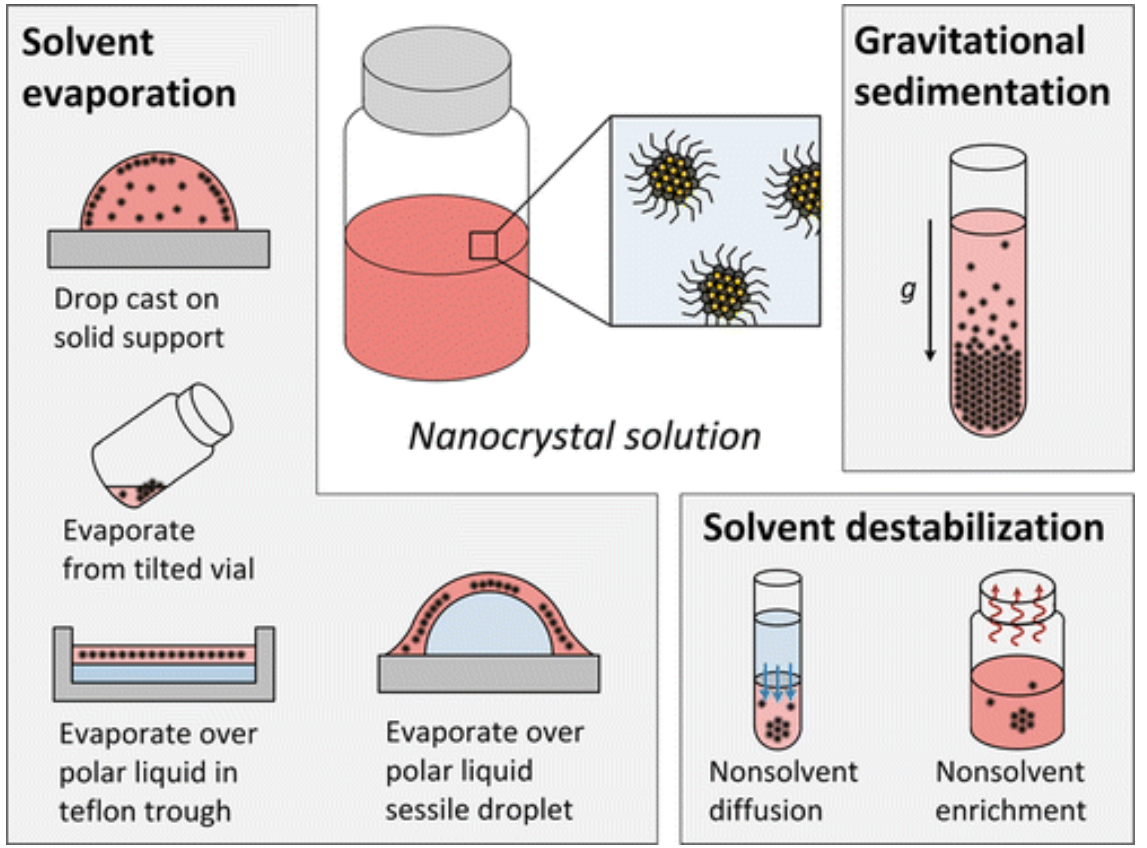

Chem. Rev. 116, 11220 (2016)

Sample systems

Nanocrystal superlattices

Gold nanospheres

- 12 nm – 30 nm diameter
- Functionalized with mixed ligands
  - Poly-ethylene glycol (PEG) with MUA spacer
  - Mixed PEGMUA / MUA ligands
- Applications: Nano-medicine, optoelectronics

Lead sulfide nanocrystals (PbS)

- “Fruit-fly” for self-assembly studies
- 3.9 nm and 7.8 nm diameter (effective)
- Oleic acid ligand
- Applications: solar cells, LED, etc. → tunable bandgap

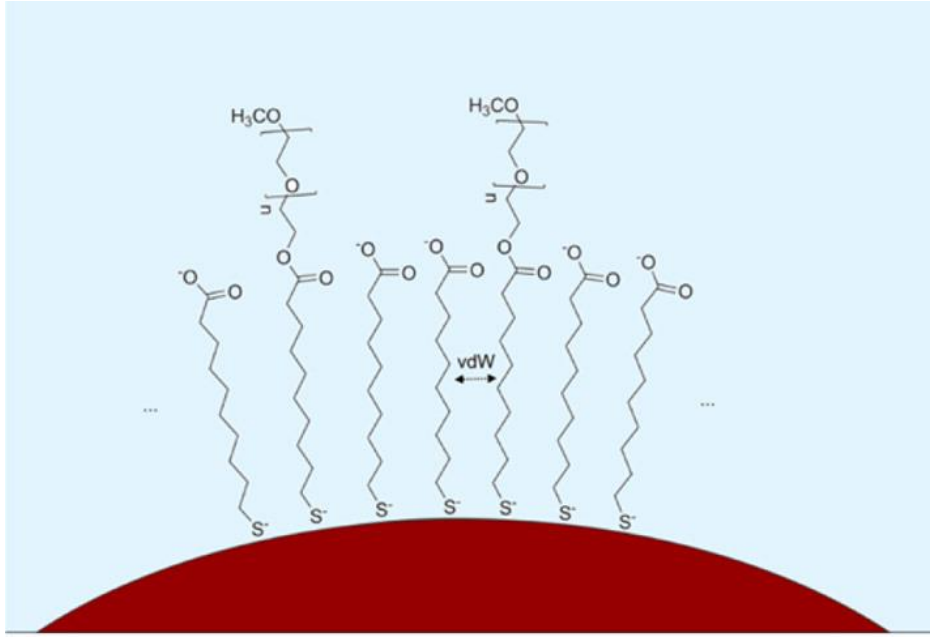

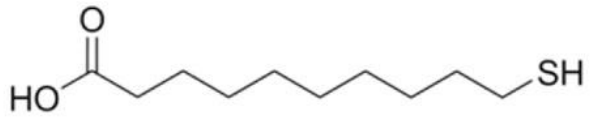

11-mercaptoundecanoic acid
MUA

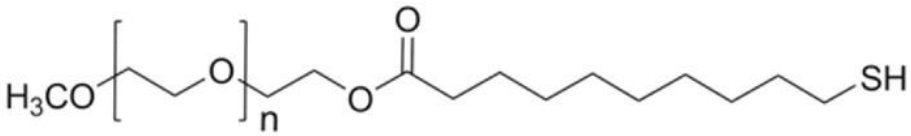

Mw~ 2000 g/mol ; n ~ 45
PEGMUA

Langmuir 32, 7897 (2016)

Self-assembled structures

Gold nanoparticles with PEG shell

- ~ 14 nm gold (radius); ~ 10 nm PEG
- Dried on silicon nitride membranes
  - $d_1 = 460 \pm 180$ nm
  - $d_2 = 190 \pm 90$ nm

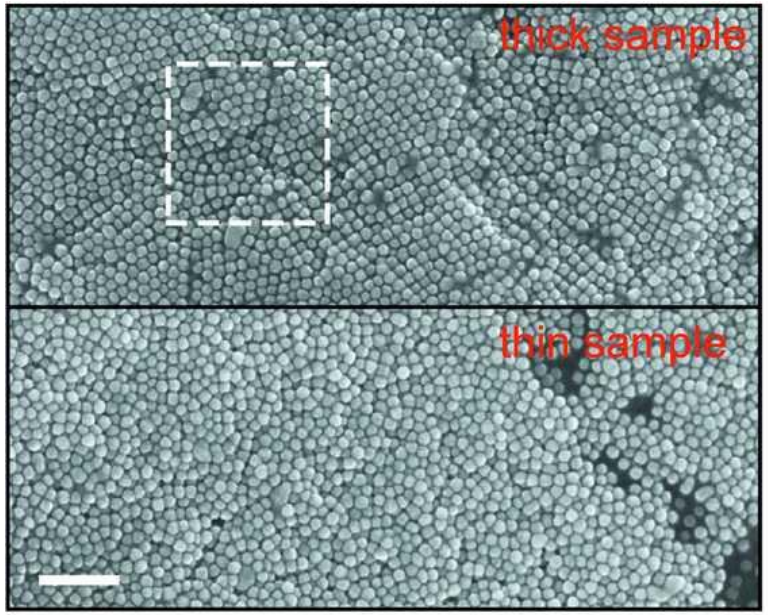

X-ray microscopy approach

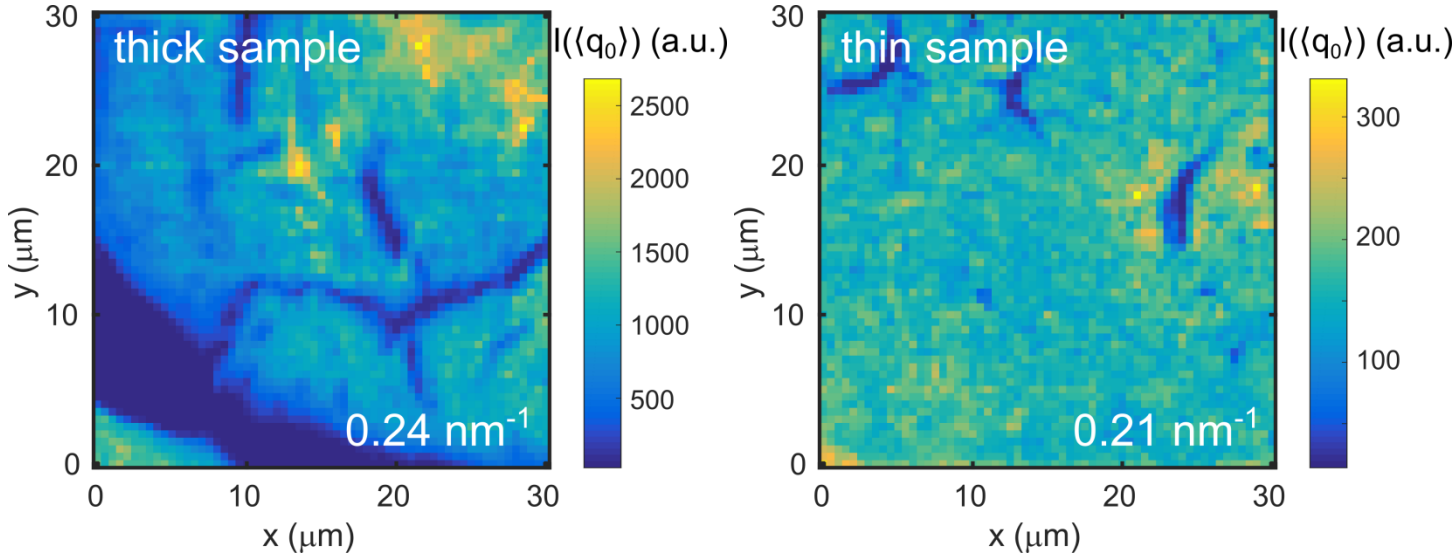

- Map of $I(q_0)$ as measure of sample thickness & averaged degree of ordering
- Sample 1: „hot spots“ & cracks
- Sample 2: more homogenous & weaker intensity
  → thinner film

FL et al. IUCrJ 5, 354 (2018)

Local order in self-assembled nanoparticle films

Spatial maps of orientational order

Ensemble-averaged XCCA

- Fourier coefficients $\Psi_\ell(q) = \langle I_\ell^2 \rangle - \langle I_\ell \rangle^2$
- Dominating 2-, 4, and 6-fold order

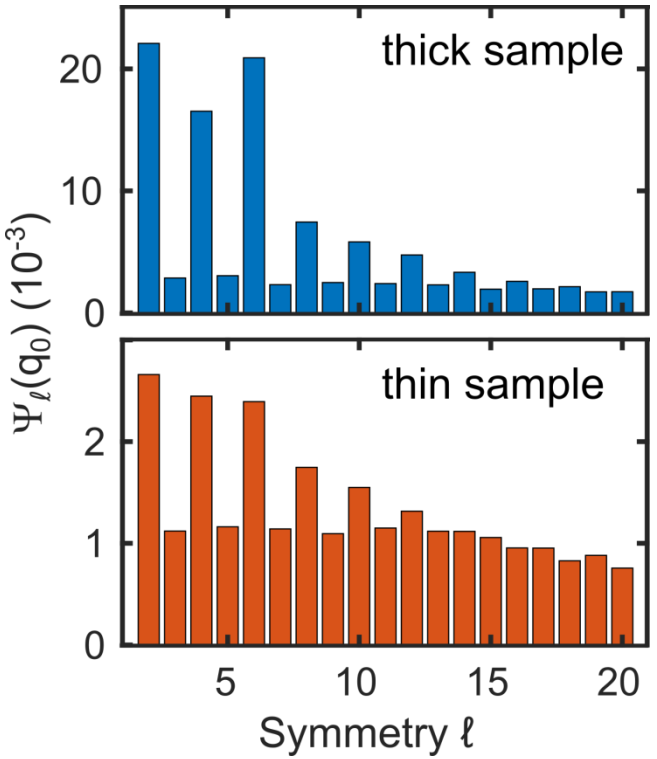

Cross-correlation microscopy

- Degree of symmetry ℓ via $I_\ell(q) = |I_\ell(q)|\exp(i\Omega_\ell(\mathrm{q}))$
- High degree of heterogeneity

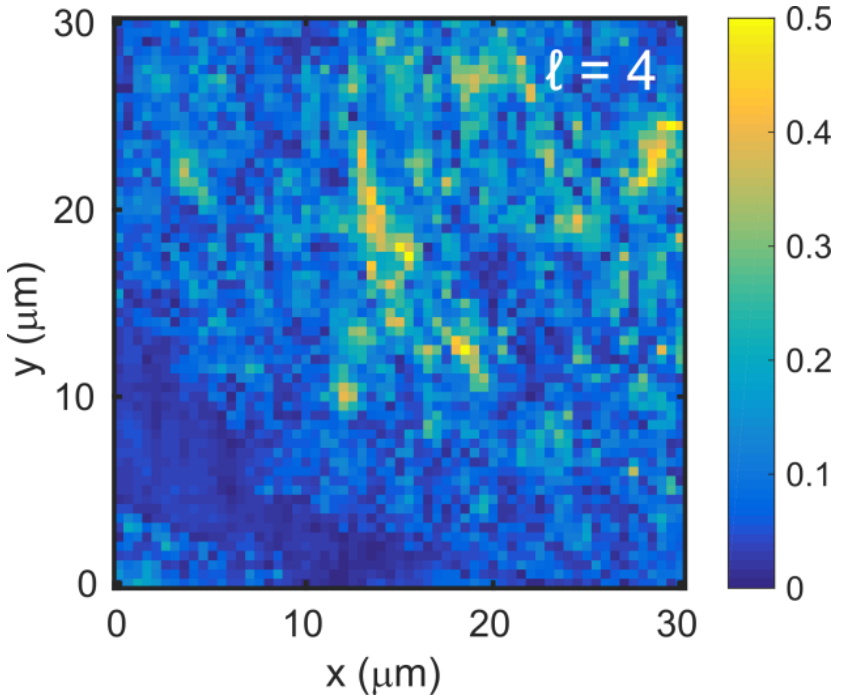

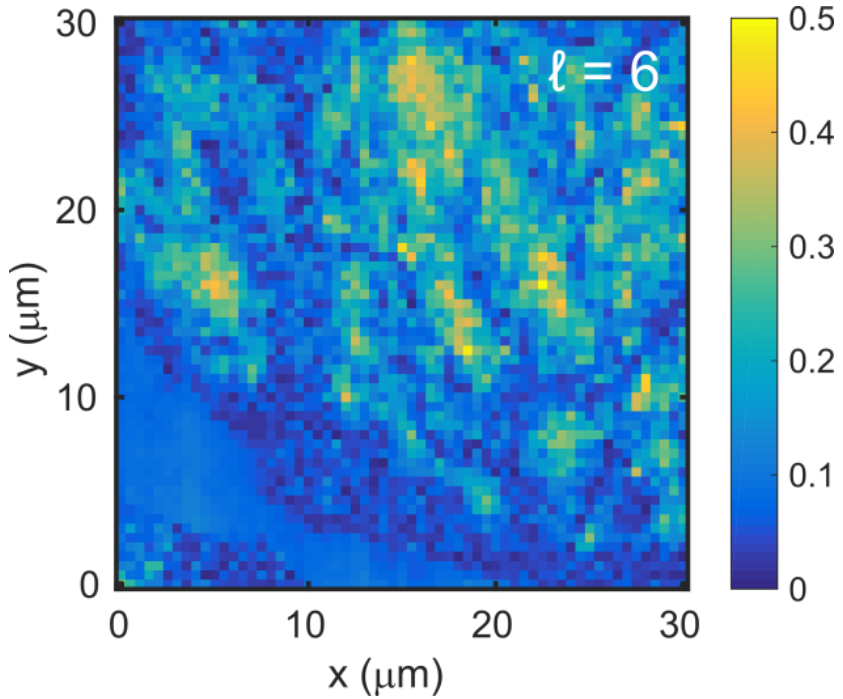

FL et al. IUCrJ 5, 354 (2018)

Local order in self-assembled nanoparticle films

Spatial maps of orientational order

- $I_\ell(q) = |I_\ell(q)|\exp\left(i\Omega_\ell(q)\right)$
- Orientation of ordered patches via phase $\Omega_\ell(q)$
- Domain size ζ_ℓ from 2D autocorrelation
- Symmetry as function of intensity ~ sample thickness: Histogram $\xi_\ell(I) = \Psi_\ell|_I$

- **Heterogeneous structure** of self-assembled colloidal films → dominating cubic and hexagonal order
- **Patch sizes** of $\zeta_4 \approx 1$ µm and $\zeta_6 \approx 3.5$ µm
- Degree of dominating order increases with **sample thickness** & shows **high variation** → high degree of heterogeneity
- **3D information** of thin films in contrast to microscopy measurements

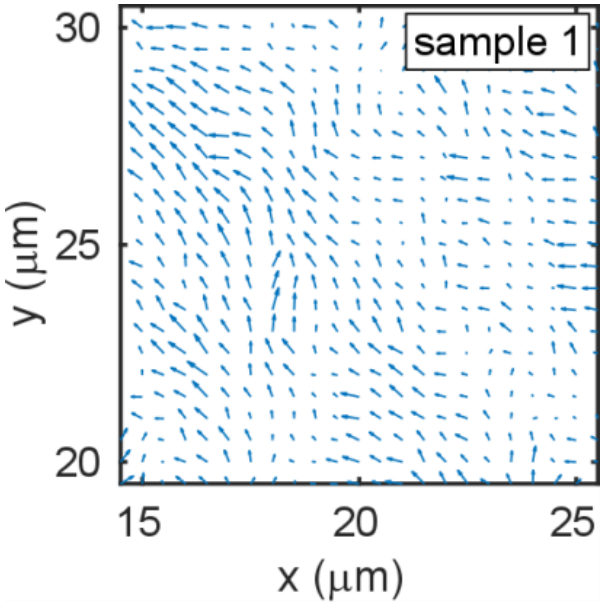

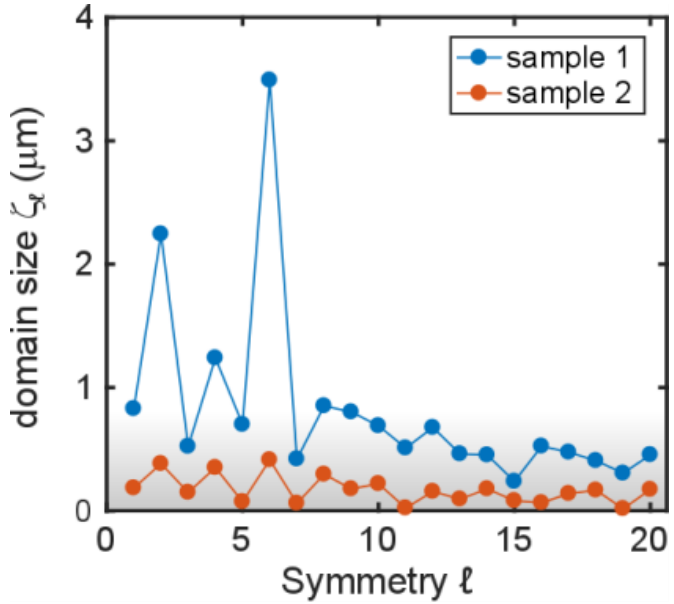

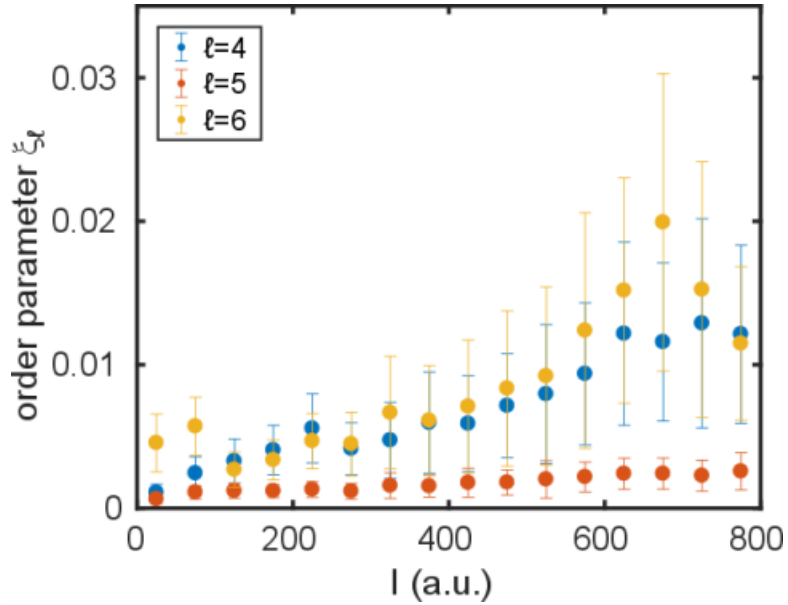

FL et al. IUCrJ 5, 354 (2018)

Role of ligand composition and salt

Symmetry-selective self-assembly

Ensemble-averaged XCCA

- Less ordered films at similar film thickness
- Reduced dominance of 4-/6-fold symmetry

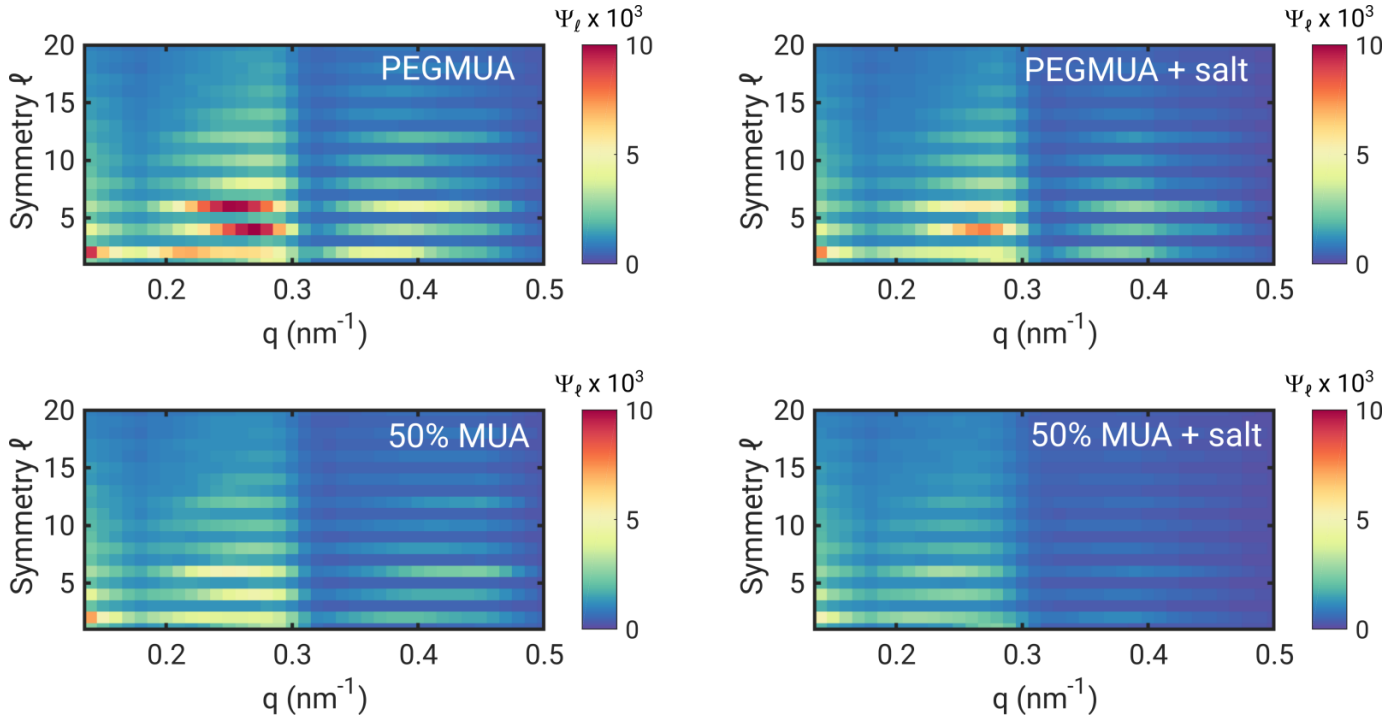

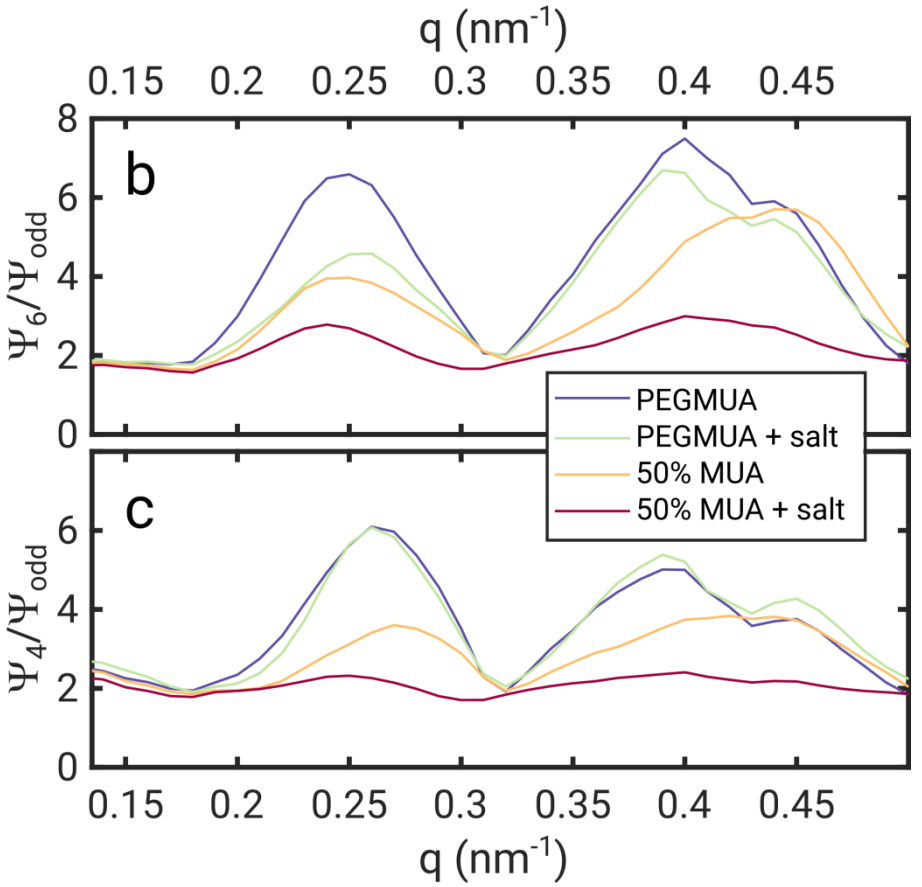

- Reduced degree of 6-fold symmetry, 4-fold symmetry unchanged in the presence of salt
- Symmetry-selective local order

FL et al. J. Appl. Cryst. 52, 777 (2019)

In-situ self-assembly

PbS nanocrystals

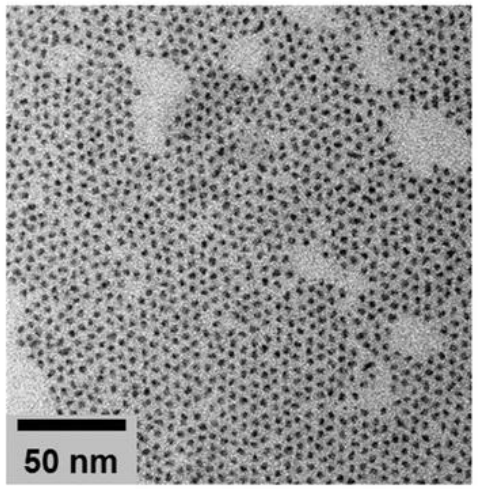

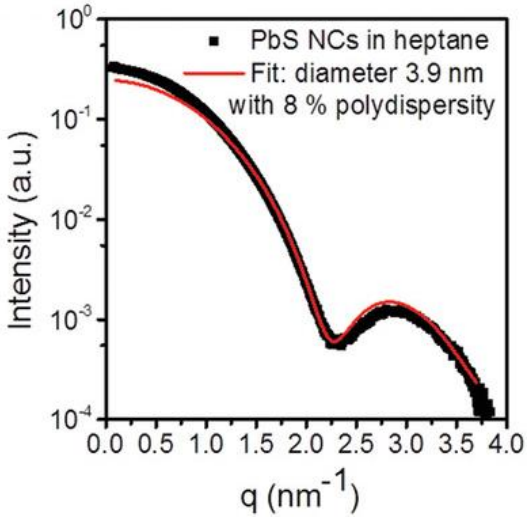

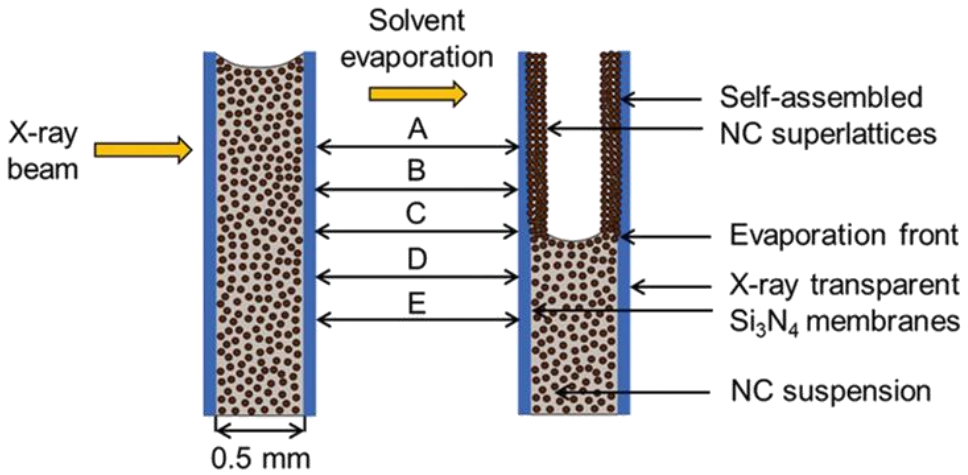

SAXS experiment at ID02

- Real-time study of self-assembly
- Controlled slow evaporation of solvent → self-assembly of nanocrystals on Si_3N_4 membranes

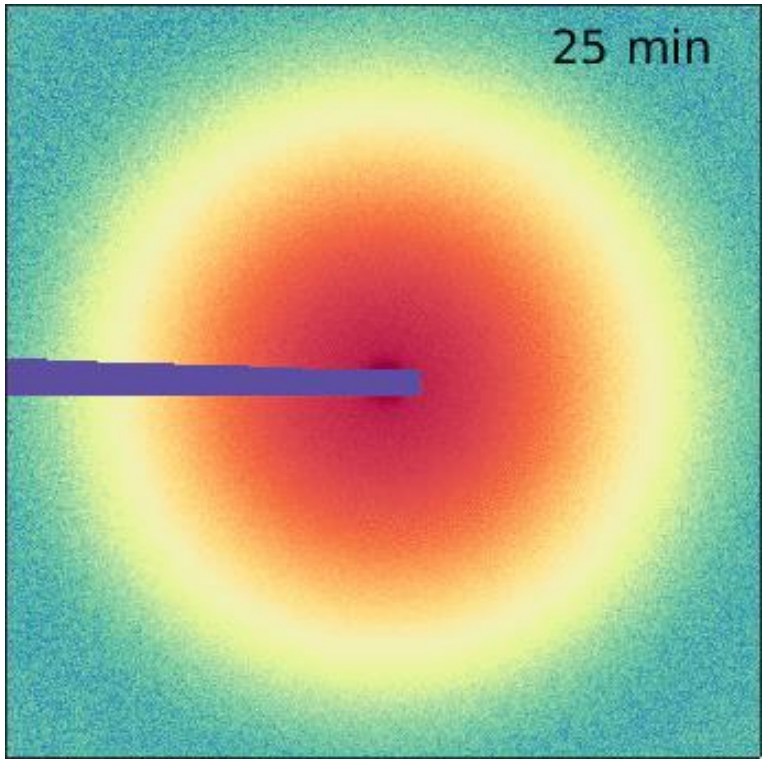

I. Lokteva et al. small 15, 1900438 (2019)

In-situ self-assembly

Implications from XCCA

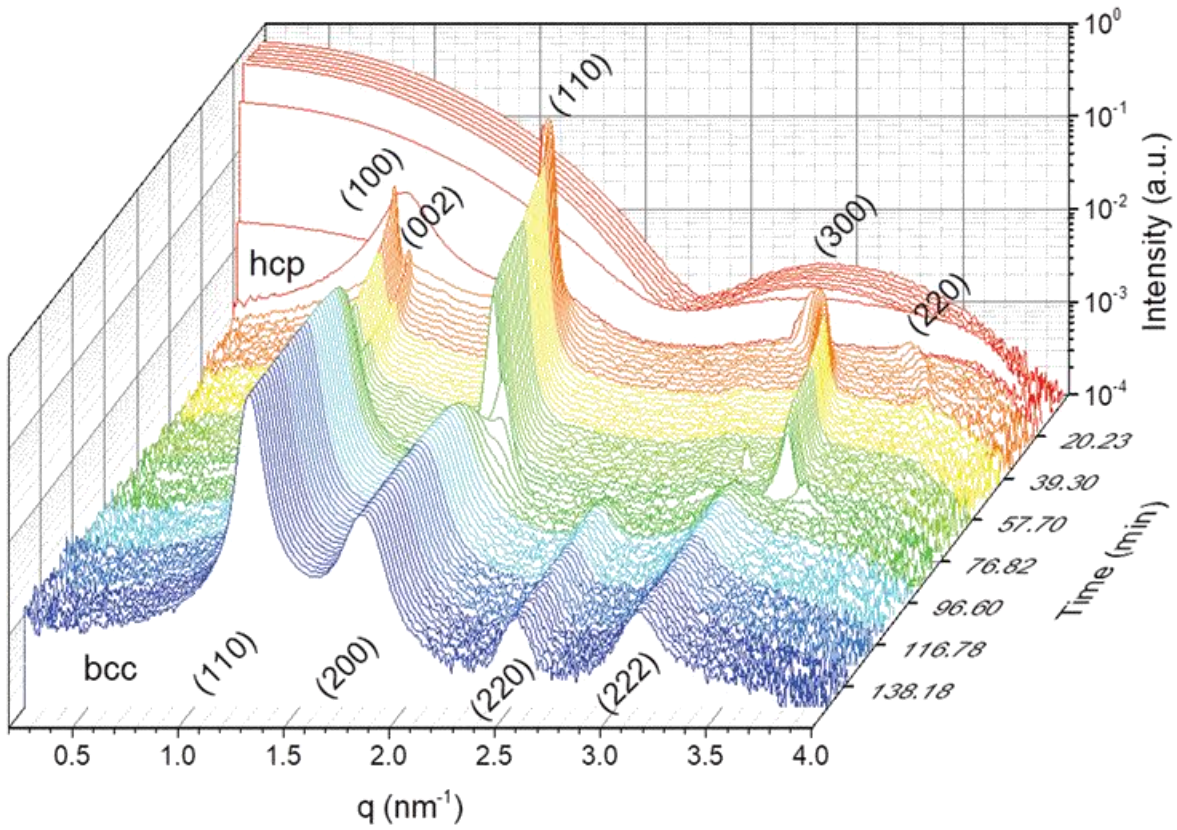

- Formation of hcp phase in solvent-saturated atmosphere → not observed at interfaces
- Transition to bcc upon complete drying

XCCA from Bragg reflections

- Symmetries support hcp and bcc phases
- Precursor of bcc (110) already in hcp state

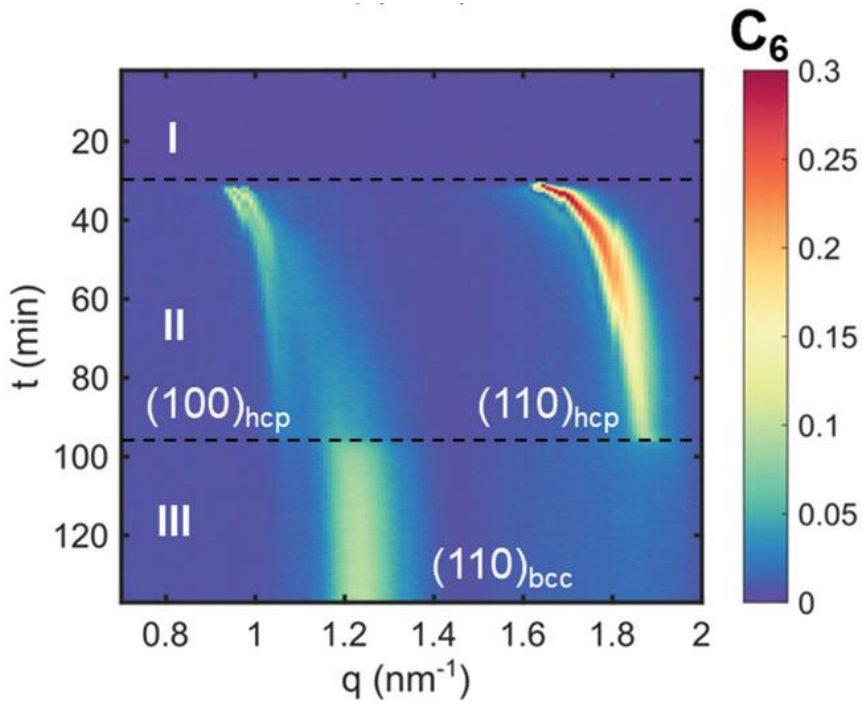

I. Lokteva et al. small 15, 1900438 (2019)

In-situ self-assembly

Faceted nanocrystals

- PbS nanocrystals with $r \simeq 7.8$ nm
  → cuboctahedral shape ($s \approx 0.5$)
- Simulations predict coexistence from hcp and bct (body-centred trigonal) phase for hard bodies

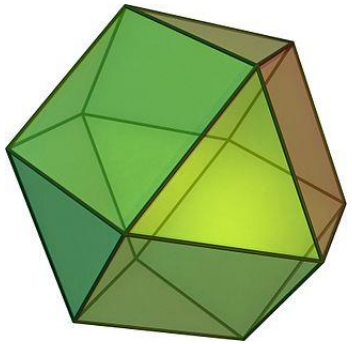

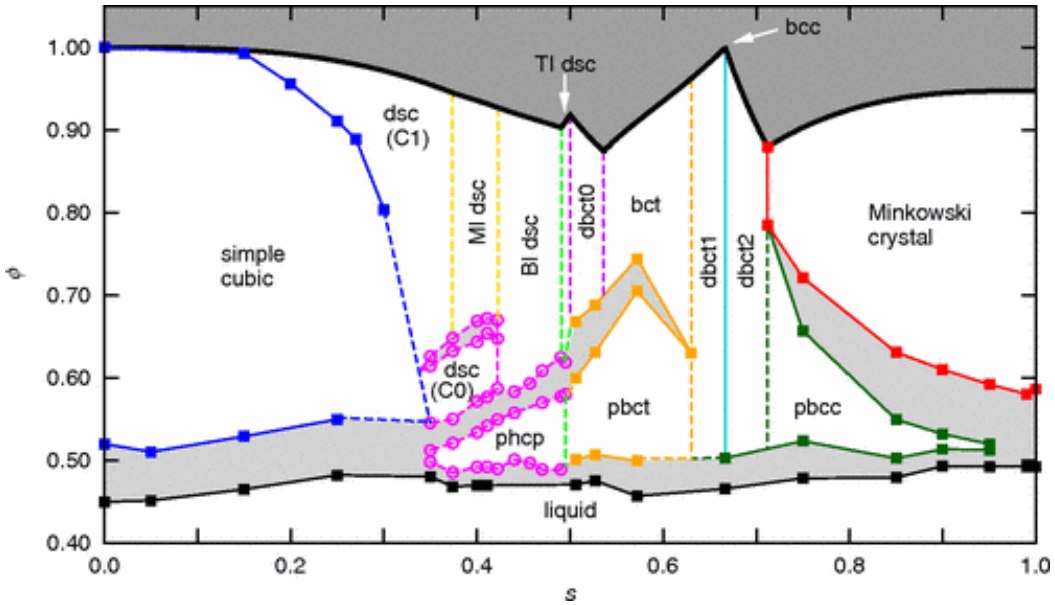

Phys. Rev. Lett. 111, 015501 (2013)

XCCA from Bragg reflections

- Multiple correlations observed for first peaks
- [redacted]

Unpublished results

I. Lokteva et al. *In review* (2019)

XCCA at ESRF-EBS

Signal-to-noise ratio

- **XPCS**: $\propto \beta I_0 \sqrt{N_{pix}} \sqrt{\tau_m}$

  → 100x coherent flux → 10^4x time

  → XPCS performance $\propto I_0^2$

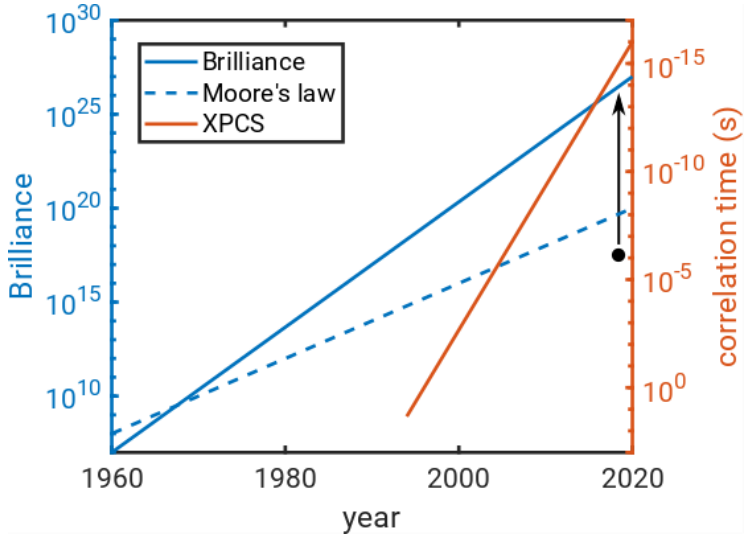

- **XCCA** (coherence-based):

  → 100x coherent flux → 100x time

  → XCCA performance $\propto I_0$

XCCA applications

- Time-resolution: in-situ processes
- XPCS & XCCA combinations – define „relevant“ correlation functions
- Crystallisation / glass transition precursors → measure of symmetries in speckle patterns
- High-energy: „extreme“ conditions

Keep in mind…

- Detectors

  → XCCA as single shot based method → tuning of exposure time

  → Need certain range of azimuth angles

- Data storage and analysis → typically need more information than in XPCS

Motivation

Spatial and dynamics heterogeneities

Spatial and **temporal heterogeneities** in the vicinity of the glass transition and crystallisation of soft matter

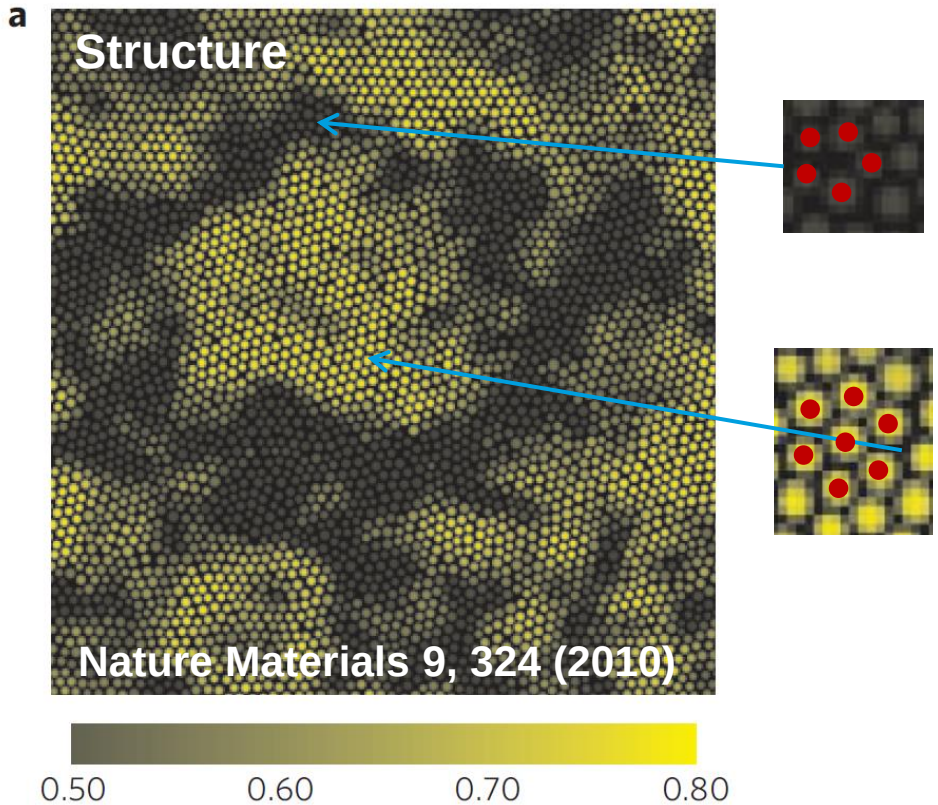

Local bond order parameter

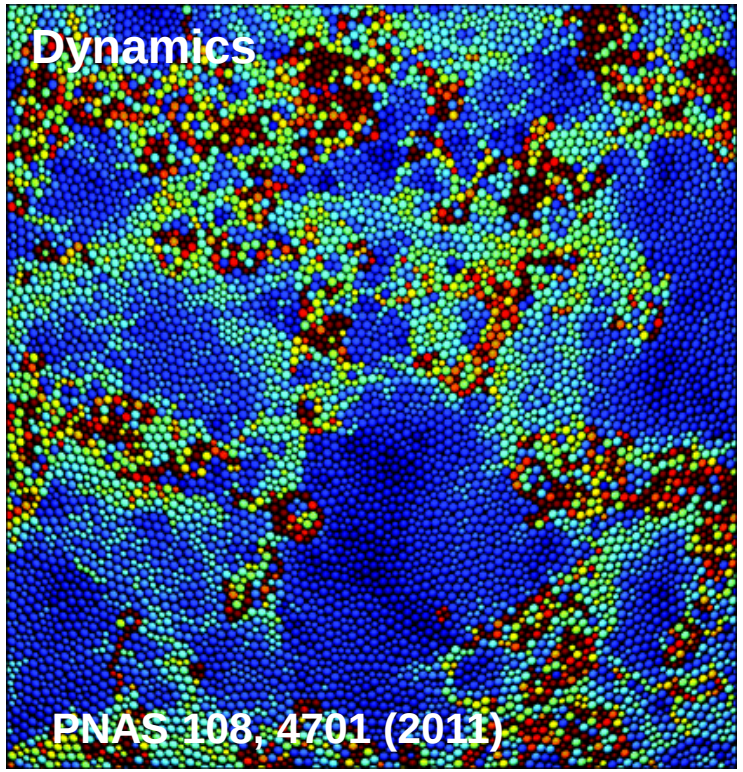

Access higher-order correlations in time (XPCS) and space (XCCA)

High-pressure studies

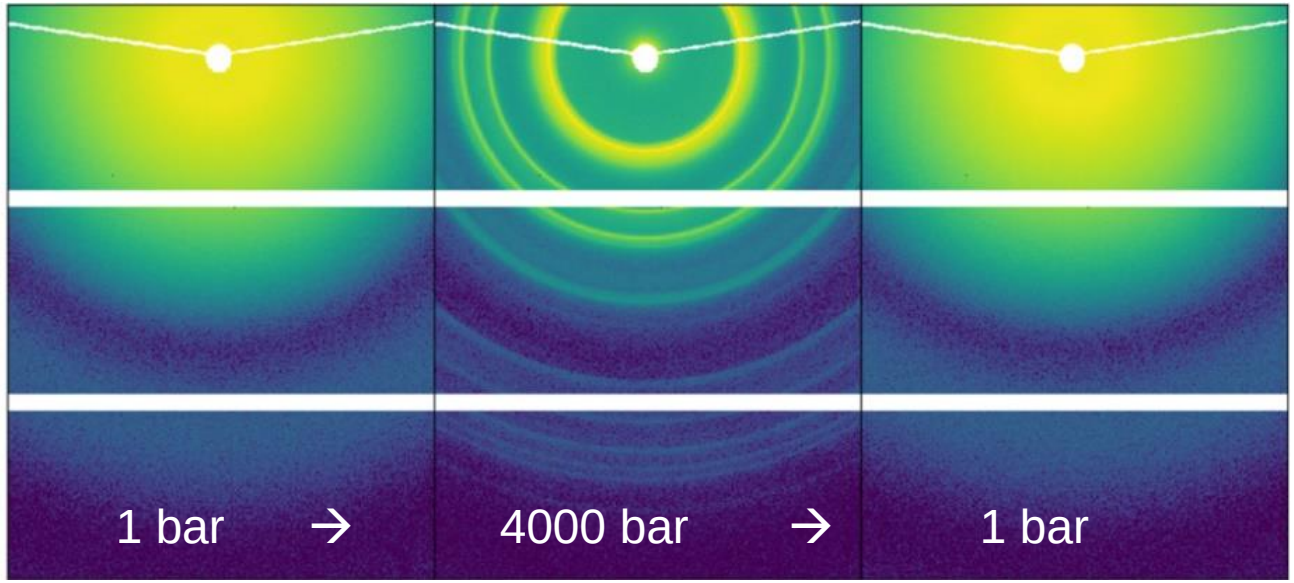

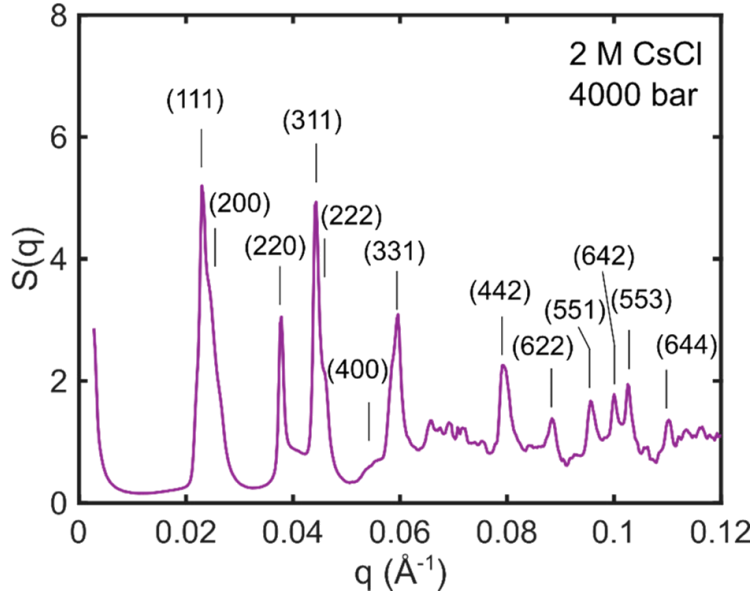

PEGylated gold particles in aqueous salt solutions

- Crystallisation at high pressures
- Phase behaviour dependent on salt concentration and type
  → role of higher-order correlation during self-assembly?

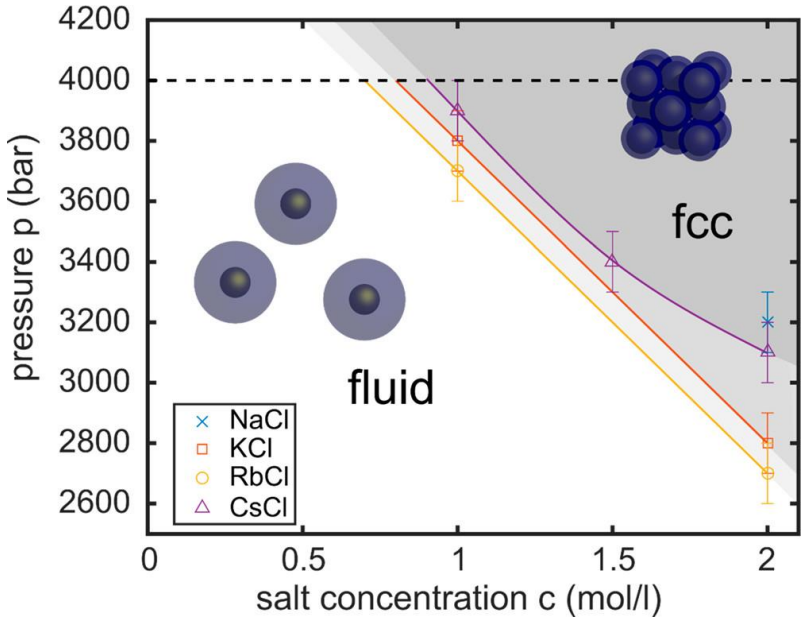

M.A. Schroer et al. J. Phys. Chem. Lett. 9, 4720 (2018)

High-pressure studies

Kinetics after pressure jumps

Structure factor after pressure jumps ($t_{jump} \approx 5$ ms)

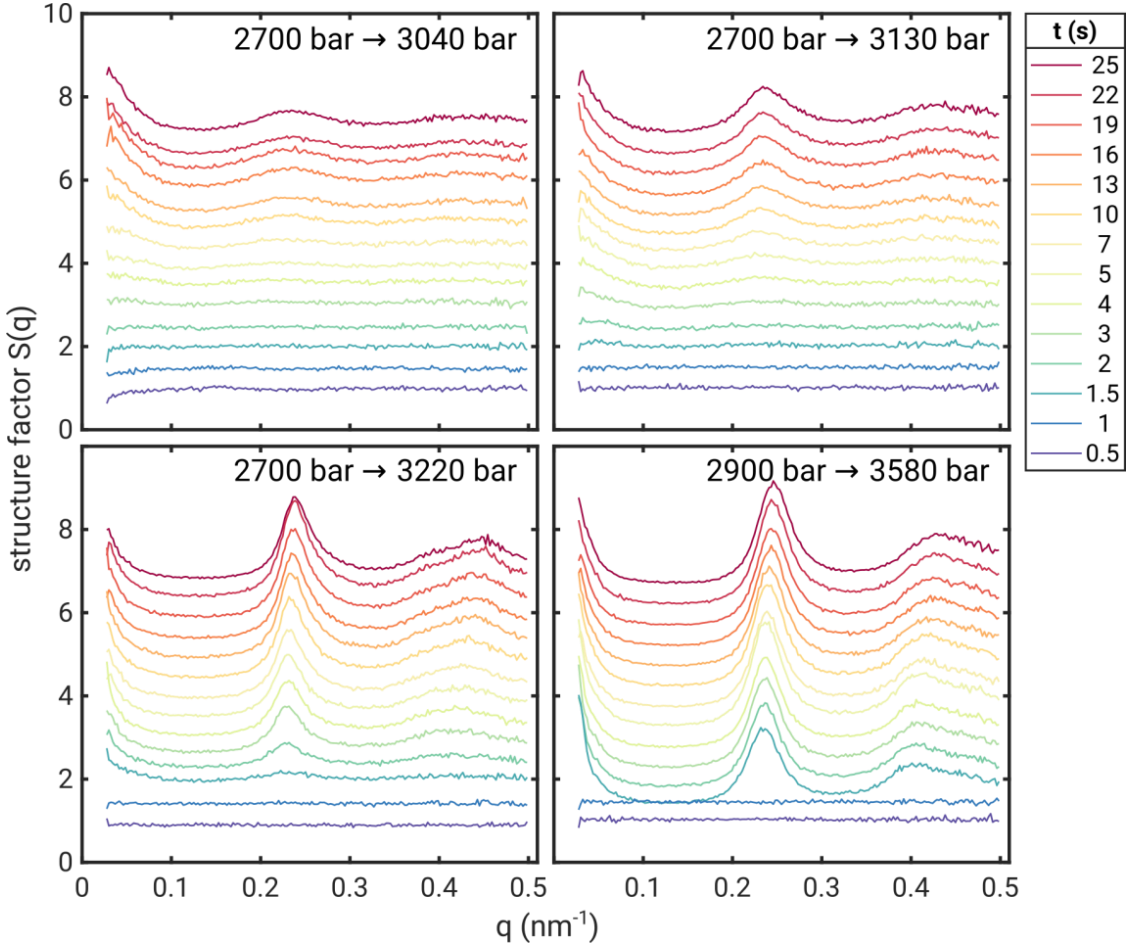

Crystallisation kinetics

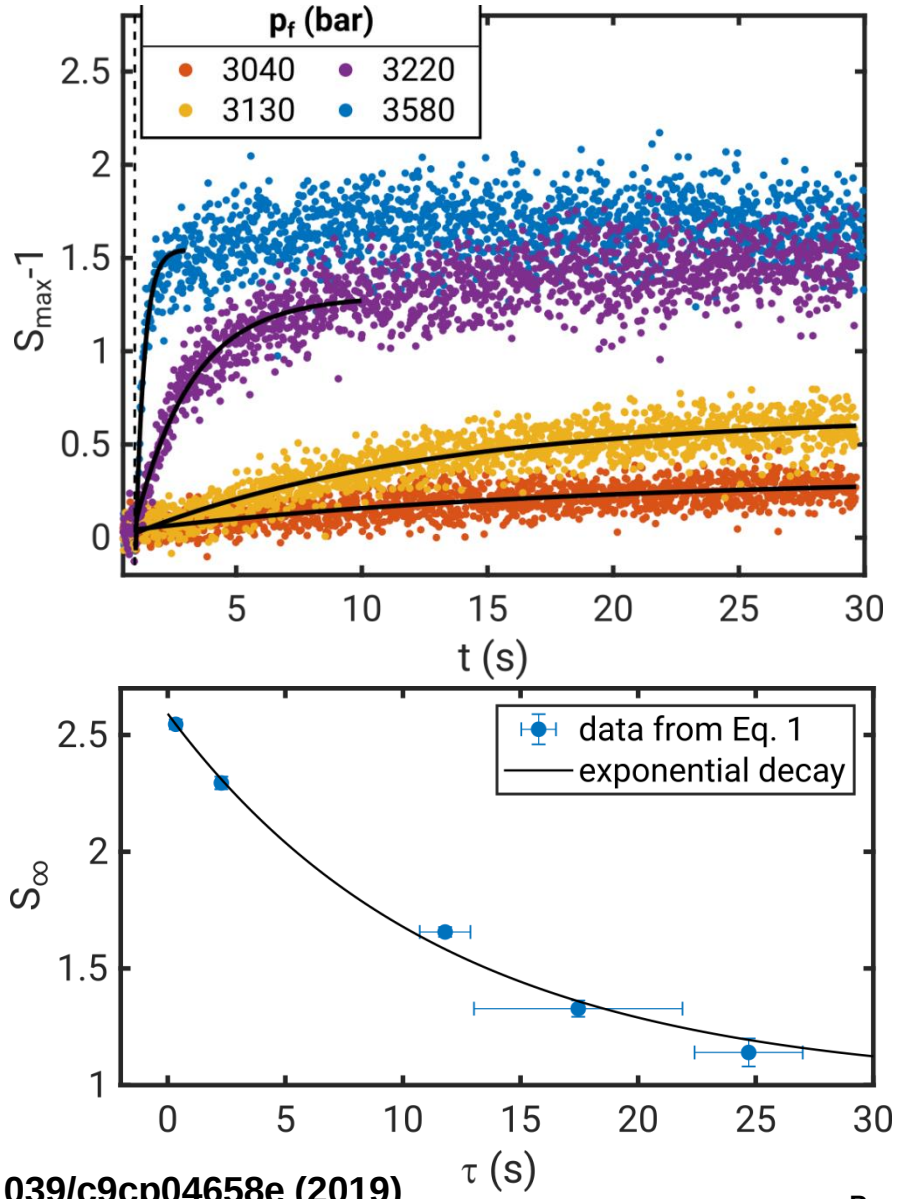

FL et al. PCCP, doi:10.1039/c9cp04658e (2019)

Acknowledgements

Coherent X-ray scattering group (FS-CXS) at DESY

- I. Lokteva, L. Frenzel, M. Koof, A. Jain, F. Dallari, J. Valerio, V. Markmann, M. Walther, and G. Grübel

Hamburg University

- F. Schulz, H. Lange

EMBL at DESY, Hamburg

- M.A. Schroer

European XFEL

- J. Möller

P10 at PETRA III – *AuNP films*

- M. Sprung, F. Westermeier, M. Osterhoff (Göttingen)

ID02 at ESRF – *PbS self-assembly*

- A. Mariani, T. Narayanan

I22 at Diamond light source – *high pressure studies*

- A.J. Smith, T. Snow, N. Terrill